

Fracture Mechanics Approach to Nondestructive Evaluation of Crack Depth in Concrete by Ultrasonic Method

T.Kamada, K.Wakatsuki, M.Asano, M.Kunieda & K.Rokugo
Department of Civil Engineering, Gifu University, Gifu, Japan

ABSTRACT: For the estimation method of crack depths in concrete by using ultrasonic techniques, the influence of micro-cracks around macro-crack tips on the propagation of ultrasonic pulses has not been clarified. In this study, crack depths in concrete beam specimens under bending loading were estimated through the ultrasonic method (ultrasonic crack depth), and were compared with the measured crack depth after dyeing. In addition, crack depths were determined by finite element analysis with the tension softening diagram, and the results were compared to those obtained through the ultrasonic method. Finally, the influence of fracture process zone(FPZ) on the evaluation of the ultrasonic crack depth was studied. As the results, the Ultrasonic Crack Depth is strongly affected by the micro cracks in FPZ, hence, it is important to consider the influence of FPZ when evaluating crack depth.

1 INTRODUCTION

The quantitative evaluation of crack depths and widths in concrete is important for the diagnosis of the structural integrity of concrete structures. The ultrasonic method is one of the nondestructive methods developed to measure the depths of cracks in concrete members. Using the characteristics of ultrasonic pulse, i.e. reflection and diffraction at interfaces between two media with different acoustic properties, this method can identify the locations and numbers of cracks (Akashi 1988).

For micro-cracks due to compressive forces, several methods to identify them by using the amplitudes and frequency characteristics of ultrasonic waves have been proposed (Iwanami et al. 1997).

For macro cracks due to tensile forces, several methods, which also use ultrasonic waves to measure the flexural crack depths of concrete members, have been studied. Most of the previous studies dealt with artificial cracks (slits) with a constant width for the whole length, and showed the depths of such cracks can be measured with accuracy (Amasaki et al. 1981, Jones 1962). Some studies, however, show that measuring the depths of flexural cracks in actual concrete structures is very difficult, if the cracks contain water inside or closed with other substances. Furthermore, actual cracks have fracture process zones around the crack tips. Although it is known that the extent of fracture process zones varies depending on the aggregate size and the characteristics of cement matrix (Otsuka et al. 1992),

little is known about the effects of fracture process zones on the accuracy of flexural crack depth measurement by the ultrasonic method. In this study, the crack depths measured by the ultrasonic method were compared with those derived from FEM analyses and those obtained from the dyeing method. Particularly, the authors focused on the effect of FPZ on the accuracy of crack depths measured by the ultrasonic wave method.

2 OUTLINE OF EXPERIMENTS

The beam specimens (with a 20 mm deep notch at the bottom-center) with the size of 100 × 200 × 800 mm (span length: 600 mm) were made. In order to vary the extent of fracture process zones, three types of specimens with different maximum aggregate sizes were also prepared: 5 mm, 15 mm, and 25 mm. In addition, specimens with another size (100 × 100 × 400 mm, span length : 300 mm, a notch depth at the bottom-center : 20mm) were produced to identify the effect of specimen size on test results. In this case, the size of aggregates used in the specimens was 15 mm. The water to cement ratio of concrete was 50% for all specimens. In the following text, the specimens with the depth of 200 mm and with the depth of 100 mm are referred to as series A and series B, respectively.

Four-point bending test was carried out, as shown in figure 1. Crack mouth opening displacement (CMOD) was measured by using a clip gauge with a

sensitivity of 1/400 mm. The magnitude of the applied loads was monitored using load cells with a capacity of 98 kN. During tests, loading and unloading were repeated where necessary to prevent brittle failure.

The locations of ultrasonic probes are shown in Figure 1. The propagation time of ultrasonic waves was measured until CMOD reached 0.27 mm for series A, and 0.17 mm for series B: the measurement was taken for every 0.01 mm increase in CMOD. The crack depth was then calculated using the Tc-To method (Jones 1962), as shown in Figure 2. The crack depth calculated in this manner is defined as "ultrasonic crack depth."

For comparison, the location of the tip of the crack (location of a node where the tensile stress reaches the tensile strength) was calculated by FEM analysis using the fictitious crack model (Hillerborg et al. 1976). The tension softening diagrams were also obtained by using the experimental load-CMOD curves in Figure 3. The crack depth calculated in this manner is defined as "analytical crack depth." An example of tension softening diagrams is shown in Figure 4, and the mesh for FEM analysis is also illustrated in Figure 5.

Dyeing method to identify crack depths was conducted for a specimen in series A, which was temporarily unloaded at times when CMOD reached 0.05 mm, 0.09 mm, 0.14 mm, and 0.20 mm. The effectiveness of the dyeing test for detecting crack depths has been proved by Goto et al. (1980). Cracks inside the specimen were dyed by injecting red ink from the notch (crack mouth). Although dyeing was conducted after the specimen had been unloaded (therefore the crack had been closed), CMOD before unloading was therefore measured to investigate its relationship with crack depth by the dyeing method. After the ink had dried, loading was resumed and

continued until failure. The fracture surfaces were then photographed, and the ratio between the colored area and the remaining area was calculated by image analysis to derive the averaged crack depth. The area of image analysis was limited to the section of 50 × 200 mm as shown in Figure 6, to coincide with the locations of the ultrasonic probe. Figure 7 is an example of the image analysis results. The maximum and minimum crack depths of this specimen (within the area of image analysis) were also calculated. The crack depth obtained in this manner is defined as "dyed crack depth."

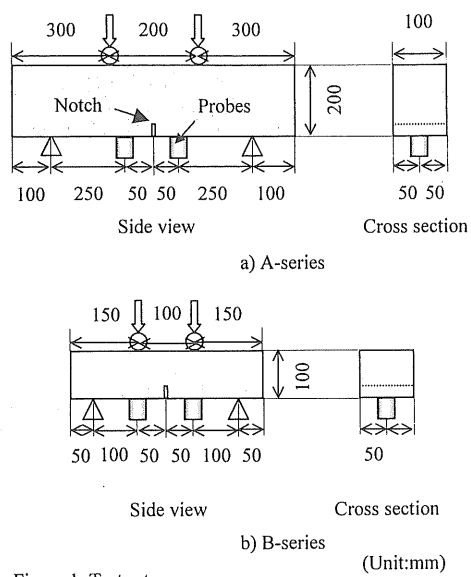
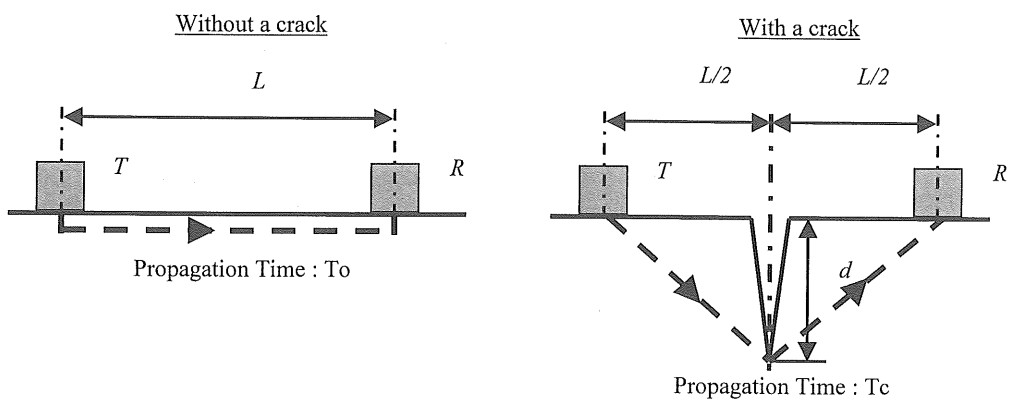


Figure 1. Test setup



$$\text{Estimated Crack Depth } d : \quad d = L / [4(Tc / To)^2 - 4]^{1/2}$$

Figure 2. T_c-T_o method

In order to investigate the extent of fracture process zones, the acoustic emission (AE) during loading was measured by the AE measuring system. The detected AE signals were amplified using a pre amplifier by 40dB and a main amplifier by 40dB, so that the total gain was 80dB. Only AE signals exceeding the threshold value of 45 dB were recorded for

analysis in the AE measuring device. In the loading tests, AE sensors were placed on the both sides of specimens to identify the two-dimensional locations of AE sources (Figure 8).

3 TEST RESULTS AND DISCUSSIONS

3.1 Extent of fracture process zones and results of AE location analysis

Figure 9 shows examples of cracks on the side of

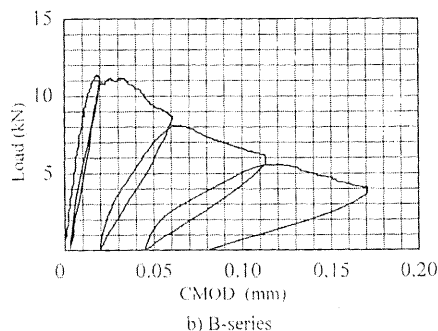
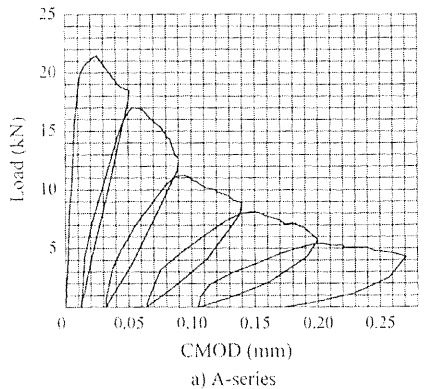


Figure 3. Load-CMOD curve

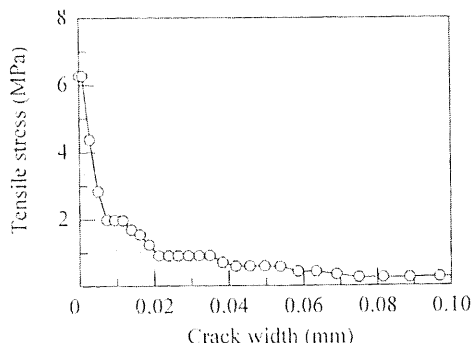


Figure 4. Example of tension softening diagram for FEM analysis

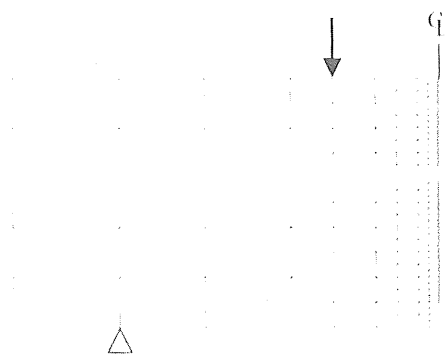


Figure 5. Mesh for FEM analysis (A-series).

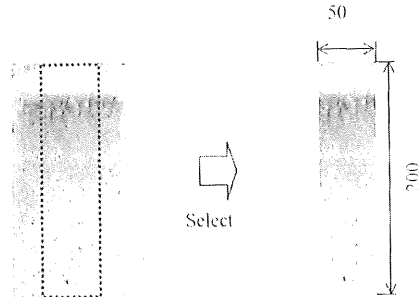


Figure 6. Measurement area of segmentation

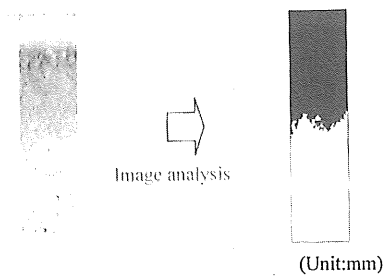


Figure 7. Image of dyed crack

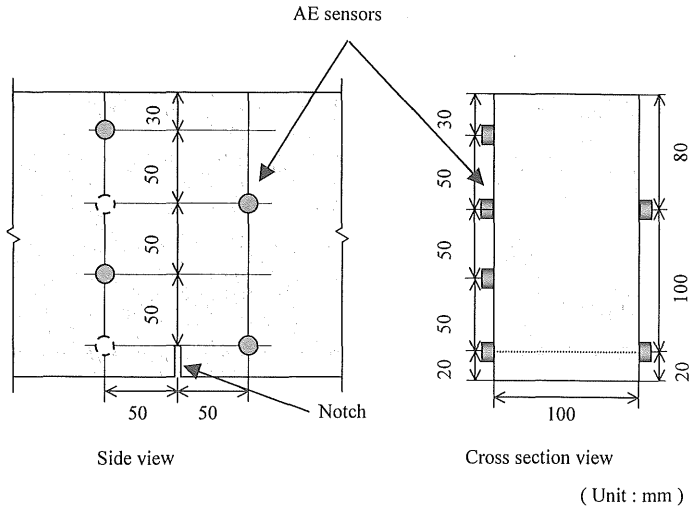


Figure 8. AE sensor locations

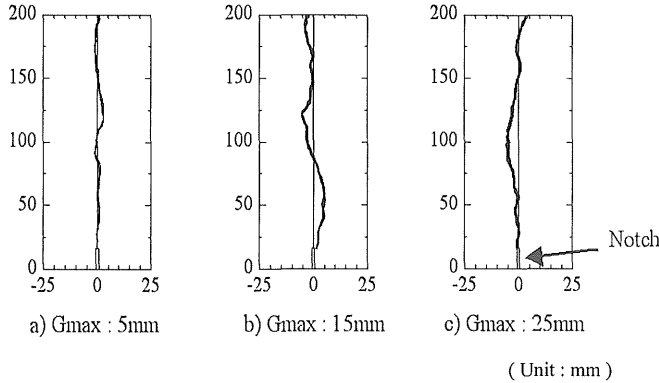


Figure 9. Cracks on specimen surface

specimens that appeared at failure. The results of AE source location analysis for specimens in series A are shown in Figure 10: the plotted points, which indicate the detected AE sources from 0.09 mm to 0.14 mm in the value of CMOD. As shown in the figure, the specimen using 25 mm aggregates has a larger area with AE sources than that of the specimen using 5 mm aggregates. Otsuka et al (1998) shows that the locations of cracks identified by the AE method have a close relation to the extent of fracture process zones.

3.2 Effects of maximum aggregate size

Figure 11 shows dyed sections of specimens with three different sizes of aggregate. The dyeing method could not be applied to some types of cracks: micro-cracks into which it is difficult for ink to

penetrate, discontinuous cracks, and cracks that have been closed after unloading. Still, it is considered that this method can be used as a means for measuring crack depths because at least areas without crack will not be dyed. The test results show that the dyed crack depths are not uniform in the section. This agrees with the findings of the study by Swartz et al (1989). This is probably because the surfaces of specimens are subject to tensile stresses due to drying-shrinkage, and the exterior sections generate more cracks than inner sections when subjected to bending stresses. The ultrasonic crack depth and the dyed crack depth at each CMOD are shown in Figure 12. The dotted line and solid line in this figure show the changes in the crack depth obtained by the ultra sonic method and by the dyeing method, respectively. The crack depth increases with the increase of CMOD regardless of the maximum size of aggre-

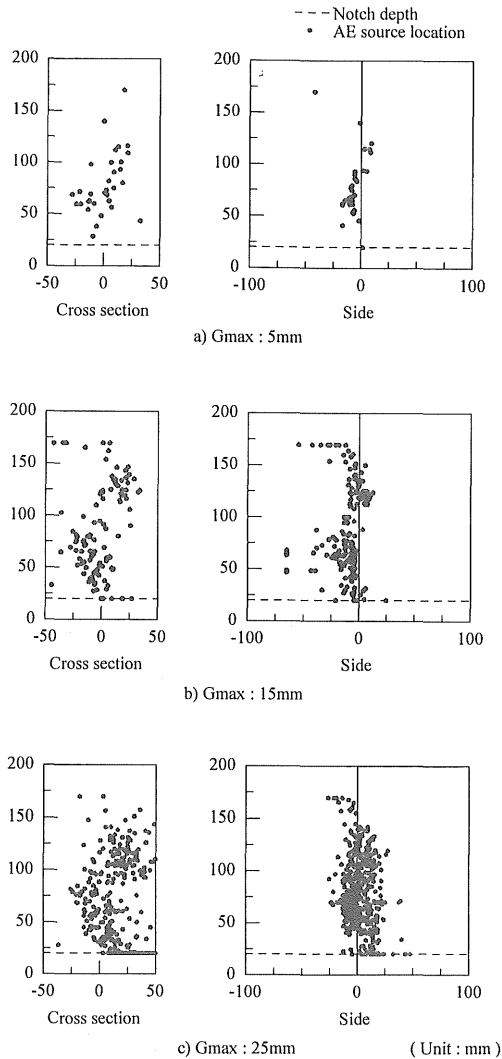


Figure 10. Location of AE sources

gates in the specimens. The differences between the maximum and minimum crack depths also increase with the increase of CMOD, and this tendency is more pronounced for specimens using large aggregates. As CMOD increases, the increment of the crack depth becomes smaller for all specimens, with those using large aggregates showing more pronounced tendency. These results also support the above-mentioned conclusion, i.e. the extent of the fracture process zones is affected by the size of aggregates.

The relationship between the ultrasonic crack depth and the dyed crack depth for each CMOD value is shown in Figure 13. Regardless of the

maximum aggregate size, the average ultrasonic crack depth is smaller than that of the dyed crack depth. On the other hand, the minimum dyed crack depth is close to that of the ultrasonic crack depth. This is probably because ultrasonic waves propagate through the shortest path when the minimum crack depth is measured. The tendency that the dyed crack depth is larger than that of the ultrasonic crack depth is more clear for the specimen using 5 mm aggregates than for specimens using 15 mm or 25 mm aggregates. Otsuka et al. (1992) investigated the characteristics of fracture process zones by X-ray photography and found that where the maximum aggregate size is 5 mm, constraint forces due to interlocking of aggregate particles are small and this rapidly creates wide and straight cracks consisting of several micro-cracks. The tests by the authors showed that the extent of the fracture progress zone in the specimen using 5 mm aggregates is relatively small, which indicates that the crack width is also small. For concrete specimens using either 15 mm or 25 mm aggregates, it is considered that the crack propagation paths are affected by the size and distributions of aggregates, and cracks propagate along the mortar-to-aggregate boundary (the weakest section in ordinary concrete) if aggregate exist ahead the paths. Cracks created in this manner will finally be distributed in wide areas of a specimen. In addition, crack widths for concrete using aggregates of these sizes are considered to be smaller than those for mortar using 5 mm aggregates. This is the probable reason that the crack depths of specimens with 15 mm or 25 mm aggregates identified by the *indirect hole method* are similar to those of specimens with 5 mm aggregates.

3.3 Effects of specimen dimension

Figure 14 shows the relationship between the ultrasonic crack depth and the analytical crack depth. For series B, the results were compared only for specimens with 15 mm aggregates. The ultrasonic crack depths are smaller than that of the analytical crack depth for both series A and B. Although the depths of cracks in an actual concrete cross section are not uniform, the fictitious crack model used in two-dimensional analysis assumed them to be uniform. In addition, the fictitious crack model assumes that cracks have large width that is sum of crack width in micro-cracks. At the tip of cracks in actual concrete, however, fracture progress zones consisting of many micro-cracks are generated and the crack surfaces contact each other. Ultrasonic waves travel though such areas and this is the probable reason why the above results were obtained. As shown by the symbol \times in Figure 14, the curve for ultrasonic crack depth plateaus when CMOD exceeds 0.11 mm. This might be because of problems related to measure-

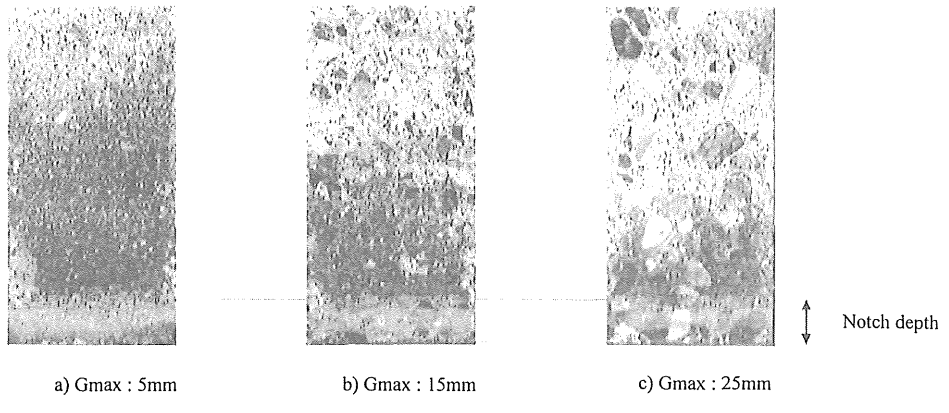


Figure 11. Examples of dyed cross section (CMOD : 0.14mm)

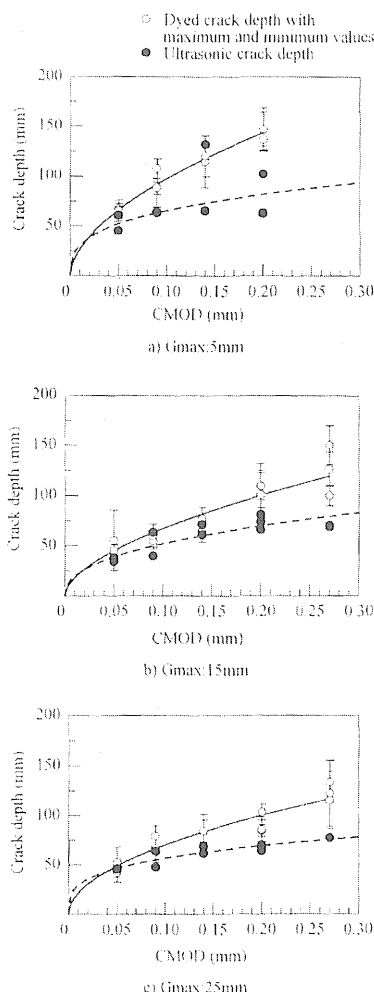


Figure 12. Dyed and ultrasonic crack depth

ment, but the actual reason for this has not yet been found. Further research and discussions are needed.

Figure 15 shows the ratio of the ultrasonic crack depth to the analytical crack depth, both excluding the notch depth. For both series, the ratio decreases with the increase of CMOD. The ultrasonic crack depth is about 40% of the analytical crack depth for series A, and about 55% for series B. The probable reasons for this are that the profile of cracks (including the extent of the fracture progress zones) change because of the difference in specimen size, and that the number of locations where crack surfaces contact each other is large for large specimens and ultrasonic waves tend to penetrate such regions. In addition, the ratios calculated from the values shown by \times in Figure 14 are given in Figure 15 for reference.

4 CONCLUSION

In this study, crack depths in concrete specimens obtained by the ultrasonic wave method, FEM analysis, and dyeing method were compared, to investigate the effects of the size of specimens and aggregates on the relationship between the extent of fracture progress zones and crack depths by the ultrasonic wave method. As a result, the following findings were obtained;

The ratio of crack depth by the ultrasonic wave method to that by analysis decreases as the size of specimens increases.

Although the extent of fracture progress zones is small for specimens using small aggregates, crack depths by the ultrasonic wave method are smaller than those by the dyeing method, since the widths of cracks are almost zero at their tips.

Crack depths by the ultrasonic wave method are affected by the extent of fracture progress zones

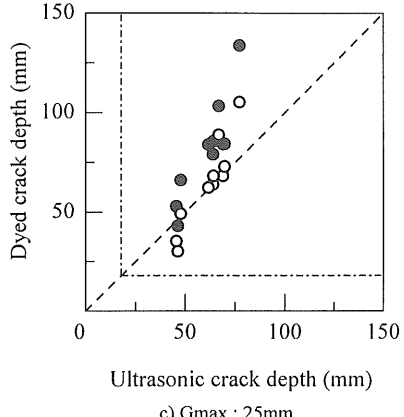
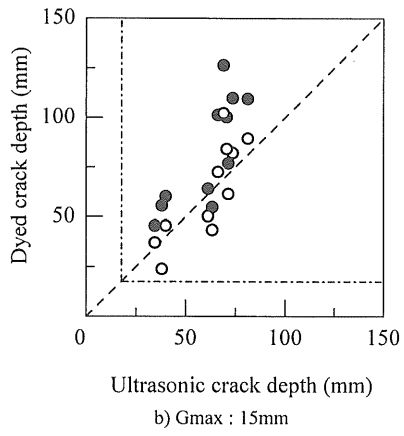
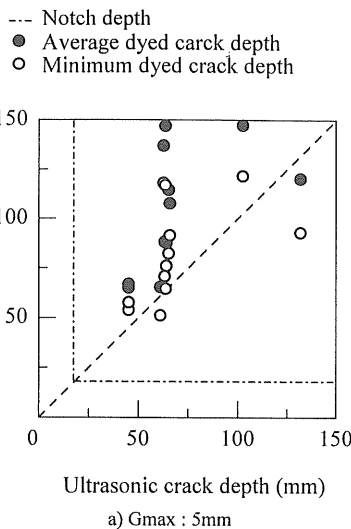


Figure 13. Relations between dyed and ultrasonic crack depths

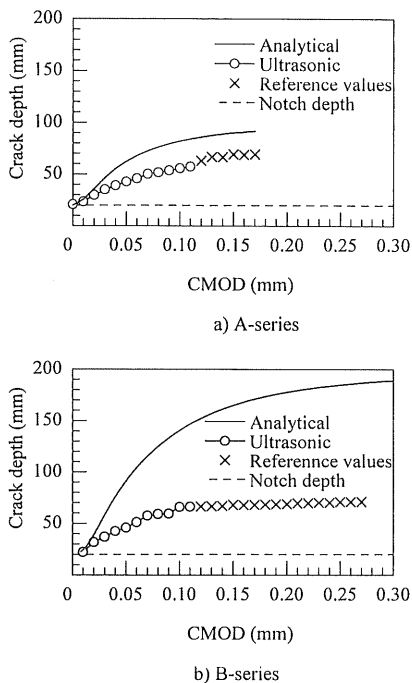


Figure 14. Relationship between ultrasonic crack depth and analytical one

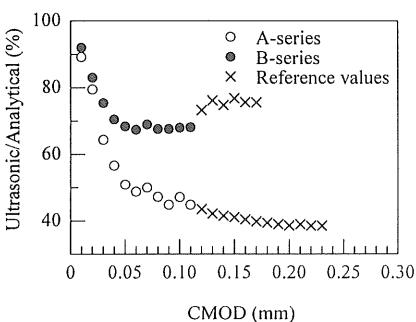


Figure 15. Ratio of ultrasonic crack depth to analytical one

which vary depending on the size of specimens and aggregates and by contact of crack surfaces. Further investigations on the effects of these factors are still needed.

REFERENCES

- Akashi, T. 1988. Studies on nondestructive testing of concrete. Proceedings of the Japan Society of Civil Engineers 390/V-8: 1-22.

- Amasaki, S. & Akashi, T. 1981. Study on a method of measurement of crack depth of concrete members by pulse velocity technique. *Proceedings of the Japan Concrete Institute 3rd conference*: 141-144.
- Goto, Y & Otsuka, K. 1980. Cracks formed in concrete around deformed bars subjected to tension, *Transactions of the Japan Society of Civil Engineers* 294: 85-100.
- Hillerborg, A., Modeer, M. & Peterson, P.E. 1976. Analysis of crack formation and crack growth in concrete by means of fracture mechanics and finite elements. *Cement and Concrete Research* 6: 773-782.
- Iwanami, M., Kamada, T. & Nagataki, S. 1997. The applicability of nondestructive testing methods to the evaluation of material deterioration in concrete. *Journal of the Japanese Society for Non-destructive Inspection* 46(3): 223-228.
- Jones, R. 1962. The non-destructive testing of concrete: 42. Cambridge University Press, London.
- Otsuka, K. 1992. Detection of fracture process zone in concrete by means of x-ray with contrast medium. *Fracture Mechanics of Concrete Structures; Proceedings of FRAMCOS-1*: 485-490. ELSEVIER APPLIED SCIENCE.
- Otsuka, K., Date, H. & Kurita, T. 1998. Fracture process zone in concrete tension specimens by x-ray and AE techniques. *Fracture Mechanics of Concrete Structures; Proceedings of FRAMCOS-3*: 3-16. AEDIFICATIO Publishers.
- Swartz, S.E. & Refai, T. 1989. Cracked surface revealed by dye and utility in determining fracture parameters. *Fracture Toughness and Fracture Energy*: 509-520. Balkem